



Article

The Spatial-Temporal Patterns and Driving Mechanisms of the Ecological Barrier Transition Zone in the Western Jilin, China

Shibo Wen ¹, Yongzhi Wang ^{1,2,*} , Tianqi Tang ³, Congcong Su ⁴, Bowen Li ², Muhammad Atif Bilal ¹ 
and Yibo Meng ⁵

¹ College of Geoexploration Science and Technology, Jilin University, Changchun 130026, China; wensb23@mails.jlu.edu.cn (S.W.)

² Institute of Integrated Information for Mineral Resources Prediction, Jilin University, Changchun 130026, China

³ College of Economics and Management, Jilin Agricultural University, Changchun 130033, China

⁴ School of Law, Zhongnan University of Economics and Law, Wuhan 430073, China

⁵ State Key Laboratory of Lunar and Planetary Sciences, Macau University of Science and Technology, Macau 999078, China

* Correspondence: wangyongzhi@jlu.edu.cn

Abstract: Land use change monitoring is a common theme in achieving sustainable development, while research on ecological barrier transition zones is relatively scarce. This study quantitatively analyzes the characteristics and patterns of land use change in Western Jilin, located in the transitional zone between the northeast forest belt and the northern sand prevention belt, from 1990 to 2020. Land dynamic change index and transition matrix are used to quantify the rates and intensities, and conversions between different land use types over time, respectively. Geodetector is adopted to analyze the impact of 12 factors on 12 types of land use change, such as using the factor detector to quantify the influence of temperature on the conversion from cropland to unused land. The results indicate that from 1990 to 2020, there have been noticeable changes in the area of various land use types in western Jilin. However, the conversion types are relatively limited, mainly involving interchanges between cropland, grassland, unused land, and water bodies. The cropland has increased by 20% overall, but 16% of that increase occurred from 1990–2000. The woodland area has steadily increased at a growth rate of 5–8% from 2000–2020, aligning with sustainable development strategies. Water bodies and grasslands are undergoing continuous recovery, and a positive growth trend is predicted to emerge by 2030. The built-up land is steadily expanding. The influencing factors vary for different types of land-use change. In a short time, policy factors play a significant role in land use, such as the implementation of the “River-lake Connection Project”, which has helped to reduce water-body fragmentation and enabled the stable recovery of water resources. However, in the long term, multiple topographic, climatic, and anthropogenic factors exhibit interactive effects in the land use change process in the area. Governments can take corresponding measures and management policies based on the influence of these factors to allocate and plan land use rationally.

Keywords: sustainable development; desertification; land degradation; Geodetector; public policies



Citation: Wen, S.; Wang, Y.; Tang, T.; Su, C.; Li, B.; Bilal, M.A.; Meng, Y. The Spatial-Temporal Patterns and Driving Mechanisms of the Ecological Barrier Transition Zone in the Western Jilin, China. *Land* **2024**, *13*, 856. <https://doi.org/10.3390/land13060856>

Academic Editors: Kathryn Sheffield, Alison L. Cowood and Mohammad Abuzar

Received: 2 May 2024

Revised: 3 June 2024

Accepted: 11 June 2024

Published: 14 June 2024



Copyright: © 2024 by the authors. Licensee MDPI, Basel, Switzerland. This article is an open access article distributed under the terms and conditions of the Creative Commons Attribution (CC BY) license (<https://creativecommons.org/licenses/by/4.0/>).

1. Introduction

One of the major challenges facing humanity today is sustainable development because the world’s population and economic activity continue to grow rapidly, putting increasing pressure on the planet’s finite resources and fragile ecosystems [1,2]. China has addressed it by establishing the “two barriers and three belts” ecological security strategy framework to enhance ecosystem stability and promote the coordinated development of economic growth and ecological protection, thus achieving the objectives of ecological civilization and sustainable development [3,4]. However, the transitional zone of the northeast forest belt and the northern sand prevention belts lie at the intersection of the

forest, grassland, and desert ecosystems. Due to the complex and dynamic geographic conditions within this ecologically diverse region, the internal structure of the region is unstable. Additionally, the area experiences low rainfall and is highly susceptible to wind and sandstorms, making the environment fragile [5,6]. Moreover, this region serves as a transitional zone between livestock farming in Western China and agriculture in Eastern China, with conflicts between agriculture and animal husbandry, particularly regarding the utilization of grasslands and cropland. Driven by economic interests, the conversion of grasslands and wetlands into cropland is common, which can result in land degradation if sustainable practices are not employed [7]. Furthermore, extensive and low-yield land use is a major cause of desertification in the region [8–10]. The irrational land-use practices and lack of coordination in land utilization have a significant impact on regional economic development and the ecological environment.

The western Jilin province is located in a typical transitional zone between the north-east forest belt and the northern sand prevention belt [11]. In the face of global climate change, rapid economic development, and numerous complex ecological challenges, it is crucial to clarify the distribution status and evolutionary patterns of land use in Western Jilin, as well as to understand the influencing factors and interactive mechanisms of land utilization in the region. This will facilitate the rational development, construction, and utilization of the area, promoting regional ecological security and sustainable development [12]. It holds significance and value to achieve green and sustainable development in the ecologically fragile transitional zone of the ecological barrier, characterized by rapid development and conflicts between human activities and the environment.

In recent years, there has been continuous progress in the study of land-use pattern evolution and its driving mechanisms. Comprehensive research has been conducted at various scales, including administrative units, watersheds, economic zones, and natural areas, covering various aspects such as ecological security and the relationship with socio-economic development [13–18]. The breadth and depth of research have been expanding and mainly focus on the following areas: (1) large-scale qualitative studies based on conceptual models [19,20]; (2) case studies and empirical analysis of land-use pattern evolution based on dynamic models [21,22]; and (3) quantitative and economic models for predicting land-use patterns to guide sustainable development [23,24]. However, most current studies on the evolution of land-use patterns and their driving mechanisms only estimate parameters in a global or average sense, lacking research that reflects spatial local variations and heterogeneity. Furthermore, in the comprehensive assessment of land use in the transitional zones of ecological barriers, there is still a lack of a comprehensive analysis of the spatiotemporal evolution process and driving mechanism indicators, such as the impact intensity of different drive factors.

Due to the inherent complexity of ecosystems, significant differences exist in different spatial and temporal scales and socio-economic development environments [25]. Therefore, the assessment of land-use patterns needs to be based on specific geographical and socio-economic characteristics, such as climate and topography, as well as socio-economic characteristics, including population and economic activities. Furthermore, to explore the mechanisms of evolution, it is necessary to conduct an in-depth analysis of the driving mechanisms behind the evolution. The driving factors of land-use pattern evolution include various aspects such as natural factors, economic factors, population factors, technological factors, and policy factors [26]. A comprehensive and accurate analysis of the driving roles of these factors is an important step in revealing the potential mechanisms of land-use pattern changes.

In this study, we aim to explore the spatiotemporal evolution process and potential driving mechanisms of land use in Western Jilin. Specifically, the main objectives of our study are as follows: (1) to analyze the spatiotemporal change process and transformation characteristics of land use in the study area, and (2) to investigate the potential driving factors behind these land use dynamics, including the roles of topography, climate, economy, and policy. Section 2 introduces the study area, data, and data preparation process.

Section 3 describes the results used in this study, including the spatiotemporal change process and transformation characteristics of the study area, as well as the potential driving mechanisms. A discussion and conclusion are presented in Sections 4 and 5, respectively.

2. Materials and Methods

2.1. Study Area

Western Jilin (121.38° E–126.11° E, 43.59° N–46.18° N) is located in the southwestern part of the Songnen Plain and the eastern part of the Horqin Grassland in China, covering approximately 48,000 km², which accounts for 27.2% of the total provincial area (Figure 1). The area includes the cities of Baicheng and Songyuan, as well as 10 subordinate county-level administrative units. The topography resembles a sieve, with higher elevation on the east, south, and west sides, and lower elevation in the northern and central parts, ranging from 96 m to 648 m. The annual average temperature is around 4–5 °C, and the rainfall ranges from 400 mm to 500 mm, decreasing from the eastern plains to the western region, with rainfall significantly lower than evapotranspiration. The region is also one of the most important black soil areas in China, with zonal soils ranging from black chernozem in the east to light black chernozem and chestnut chernozem towards the west [27]. Situated in the transitional zone between agriculture and animal husbandry in Northern China, the area represents a typical semi-arid and semi-humid region. It is an important agricultural and animal husbandry-production base, as well as an energy-production base in the northeastern region. Dryland farming, relying primarily on natural precipitation with limited irrigation, is the predominant agricultural practice. The major crops cultivated include food grains such as corn, soybeans, wheat, and sorghum, as well as economic crops like vegetables and melons, which to some extent satisfy the local and regional food demand and market supply. Livestock husbandry, focusing on cattle, sheep, and horses, is a crucial livelihood source for the local rural residents. According to the statistics from the end of 2022, the total population of the region is approximately 3.7 million. With economic development and regional expansion, the area faces serious challenges such as soil salinization, desertification, grassland degradation, wetland shrinkage, and unreasonable land use structure. These issues have posed significant obstacles to local development [28–31].

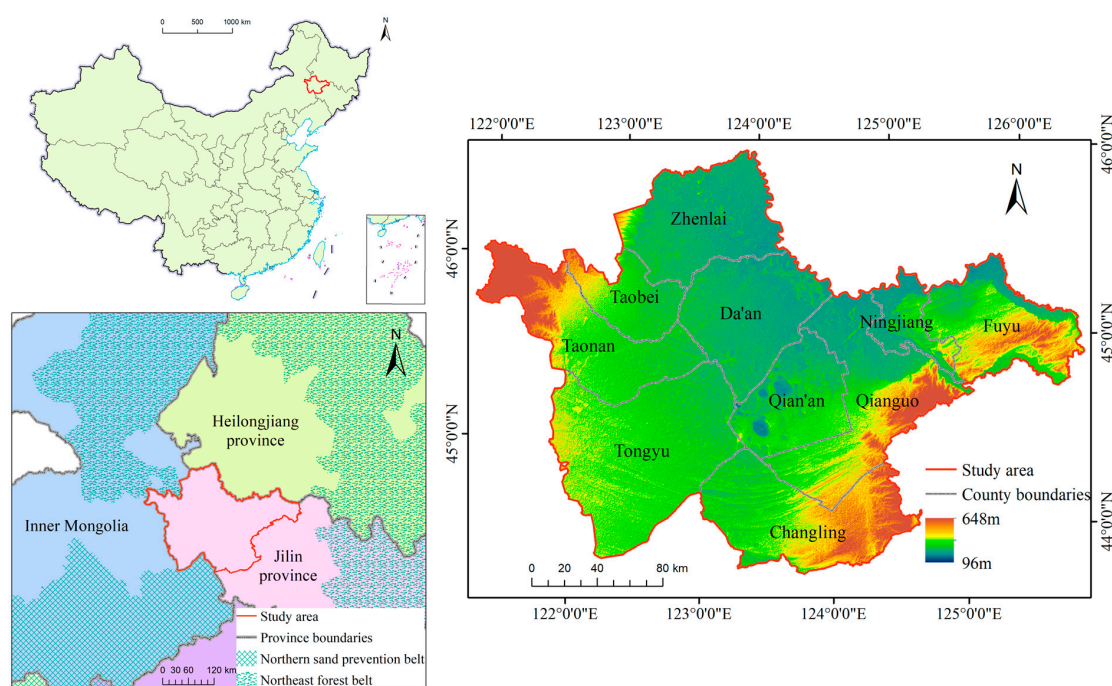


Figure 1. Location (left) and administrative division (right) of the study area in China, (Source of elevation: Geospatial Data Cloud (<https://www.gscloud.cn/>), accessed on 20 February 2024)).

2.2. Data and Preprocessing

Table 1 presents the basic dataset information and sources used. The land-use data were obtained from the land-use remote-sensing monitoring dataset with a 30 m resolution covering the years 1990, 2000, 2010, and 2020, released by Resource and Environment Science and Data Center (<https://www.resdc.cn>, accessed on 28 February 2024). These land-use data were generated based on Landsat 8 satellite imagery, through manual visual interpretation, and underwent rigorous radiometric and geometric corrections, with an accuracy of over 90% [32,33]. The land-use data were then reclassified into six categories: cropland, woodland, grassland, water body, built-up land, and unused land (unused land primarily refers to areas that are currently not utilized or difficult to utilize, such as sandy areas, saline–alkali land, and so on), based on the classification standard of the Chinese Academy of Sciences Land Resource Classification System [34–36].

To investigate the driving mechanisms behind land use changes in the area, 12 geographical spatial covariates were selected from a larger set of potential covariates based on their uniqueness, spatial resolution, data availability, and relevance. These covariate datasets were labeled as X1, X2, . . . , X12. Broadly, these covariates can be categorized into three groups: topography, climate, and economics. The topography covariates included DEM, slope, and aspect. The climate covariates consisted of annual rainfall, average annual temperature, soil moisture, and aridity index. The DEM (Digital Elevation Model) and average temperature data were obtained from the Global Climate and Weather Database (<https://worldclim.org/data/index.html>, accessed on 28 February, 2024) with a spatial resolution of 30'' [37]. The slope and aspect data were derived from the DEM. The annual rainfall data were sourced from the Global Rainfall Climatology Centre Dataset with a spatial resolution of 1° [38]. The soil moisture dataset with 15' resolution was acquired from the Science Data Bank (<https://www.scidb.cn/>, accessed on 25 May 2024) [39]. The aridity index was accessed from the Plant Science Data Center (<https://www.plantplus.cn/doi/doi.org/10.6084>, accessed on 25 May 2024), with a resolution of 30'' [40]. The economic covariates comprising GDP (Gross Domestic Product), population size, agricultural population size, livestock population, and urbanization level, were collected from the China Statistical Yearbooks (<http://www.stats.gov.cn/>, accessed on 28 February 2024) for the years 2010 and 2020, as well as the Jilin Statistical Yearbook (<http://tjj.jl.gov.cn/index.html>, accessed on 28 February 2024). Additionally, policies related to land-use change in the study area were manually collected and analyzed to examine the correlation between land-use change and policy changes [41].

To ensure data consistency and overcome unit differences between factors, all raster data were resampled to a 30 m resolution using the nearest neighbor method in ArcMap 10.8 and projected in the Krasovsky_1940_Albers (ESPG:7024) coordinate system. GDP data were converted to US dollars using the current exchange rates. Based on R 4.4.0 environment with Rstudio 4.4.0, and the `optdisc` function from the `GD` package 10.3 [42], the system automatically calculated the optimal discretization method and classification from the six discrete methods: equal, natural, quantile, geometric, Sd (standard deviation), and manual, and applied the discretization to each data type accordingly.

2.3. Methods

2.3.1. Land-Use Change Index

Land-use changes demonstrate distinct spatial distributions under the influence of multiple factors. Consequently, the changes in various land-use types within a specific time and space become a complex process. The land-use change index can capture the variations in land-use change patterns across different land types or periods within the same region. It highlights the level of intensity in land utilization. A higher dynamics index indicates greater land-use change activity for a specific land cover type under conditions. The individual land-use change index (M) (Equation (1)) enables the examination of dynamic

changes associated with a specific type, while the comprehensive land-use change index (LC) (Equation (2)) facilitates the study of the overall intensity of land-use changes [32].

$$M = \frac{U_b - U_a}{U_a} \times \frac{1}{T} \times 100\% \tag{1}$$

$$LC = \sum_{ij}^n \frac{\Delta L_{U_{i-j}}}{L_{U_i}} \times \frac{1}{T} \times 100\% \tag{2}$$

where T is the study period and U_a and U_b represent the area of a certain land-use type at the initial and final stages of the period, respectively. L_{U_i} represents the area of the initial land-use type i at the beginning of the study period, and $\Delta L_{U_{i-j}}$ represents the area of land-use type i converted into other types, i is the number of types ($i = 1, \dots, n$).

Table 1. The data used in this study.

Code of Factor	Dataset	Year	Initial Resolution	Sources	
1	-	Land use data	1990, 2000, 2010, 2020	1''	Resource and Environment Science and Data Center (https://www.resdc.cn , accessed on 28 February 2024)
2	X1	DEM	1990, 2020	30''	Global Climate and Weather Database (https://worldclim.org/data/index.html , accessed on 28 February 2024)
3	X2	Slope	1990, 2020	30''	Calculate from DEM
4	X3	Aspect	1990, 2020	30''	Calculate from DEM
5	X4	Annual rainfall	1990, 2020	1°	Global Rainfall Climatology Centre dataset [38]
6	X5	Average annual temperature	1990, 2020	30''	Global Climate and Weather Database (https://worldclim.org/data/index.html , accessed on 28 February 2024)
7	X6	Soil moisture	1990, 2020	15'	Plant Science Data Center (https://www.plantplus.cn/doi/doi.org/10.6084 , accessed on 25 May 2024)
8	X7	Aridity index	1990, 2020	30''	Science Data Bank (https://www.scidb.cn/ , accessed on 25 May 2024)
9	X8	GDP	1990, 2020	-	China Statistical Yearbooks
10	X9	Population size	1990, 2020	-	(http://www.stats.gov.cn/ , accessed on 28 February 2024)
11	X10	Agricultural population size	1990, 2020	-	Jilin Statistical Yearbook
12	X11	Livestock population	1990, 2020	-	(http://tjj.jl.gov.cn/index.html , accessed on 28 February 2024)
13	X12	Urbanization level	1990, 2020	-	
14	-	Relevant policies	1990–2020	-	

2.3.2. Land-Use Transfer Matrix and Trajectories

The land-use transfer matrix (Equation (3)) originates from the quantitative description of system states and state transitions in system analysis [43]. It can quantitatively reflect the structural characteristics among different land-use types and reveal the transition rates between different land-use types.

$$S_{ij} = \begin{bmatrix} S_{11} & S_{12} & \dots & S_{1n} \\ S_{21} & S_{22} & \dots & S_{2n} \\ \dots & \dots & \dots & \dots \\ S_{n1} & S_{n2} & \dots & S_{nm} \end{bmatrix} \tag{3}$$

where n represents the number of land-use types, S_{ij} means the area of land conversion from type i to type j ($i, j = 1, 2, 3, \dots, n$). The calculation of the land-use change index and the land use transfer matrix is completed with the help of ArcGIS 10.8.

2.3.3. Driving Factors Detection

Geodetector is an emerging statistical model used to quantitatively identify the driving factors that influence these variations [44]. Geodetector analysis can reflect the similarities within the same area and the differences between regions and reveal the spatial heterogeneity of geographic units and related driving factors [45].

Geodetector includes four modules: factor, risk, ecological, and interaction detector. The factor detector can identify the spatial variation of a factor on a dependent variable and determine the importance of the factor’s influence. The interaction detector can identify whether two factors interact or act on the dependent variable separately, and it determines the strength and direction of the interaction. The risk detector can derive the optimal range of the factors considered. Therefore, in this study, the factor detector (Equation (4)) was used to quantitatively detect the influence of factor X on the spatial variation of Y. The interaction detector was used to identify the strength of the interaction between two factors. The risk detector was used to derive the optimal range of factors. A vector network covering the study area was established, where each grid in the network is 3 km × 3 km in size. The ratio of the number of land use change pixels to the total number of pixels in each grid was used as the network central attribute value (Y) to determine the intensity of land use change and analyze the driving mechanisms. Similarly, the average values of each driving factor in each grid have also been sampled to the grid center as the X. The types of land use change are shown in Table 2.

$$q = 1 - \frac{1}{N\sigma^2} \sum_{h=1}^L N_h \sigma_h^2 \tag{4}$$

where q is the explanatory index or determinism of the factor X to land-use change type Y, and it ranges within [0–1]. A larger q indicating a greater explanatory power of the X on Y. h is the number of land-use changes ($h = 1, \dots, n$); L is the number of classifications of land-use change Y or factor X; N is the number of units of Y in the study area; σ_h^2 are the variances of Y in the study area.

Table 2. Type of land-use change.

	Connotation
1	Cropland → woodland
2	Cropland → grassland
3	Cropland → built-up land
4	Woodland → cropland
5	Woodland → grassland
6	Woodland → built-up land
7	Grassland → cropland
8	Grassland → woodland
9	Grassland → built-up land
10	Water body → cropland
11	Cropland/woodland/grassland/water → unused land
12	Unused land → cropland/woodland/grassland/water

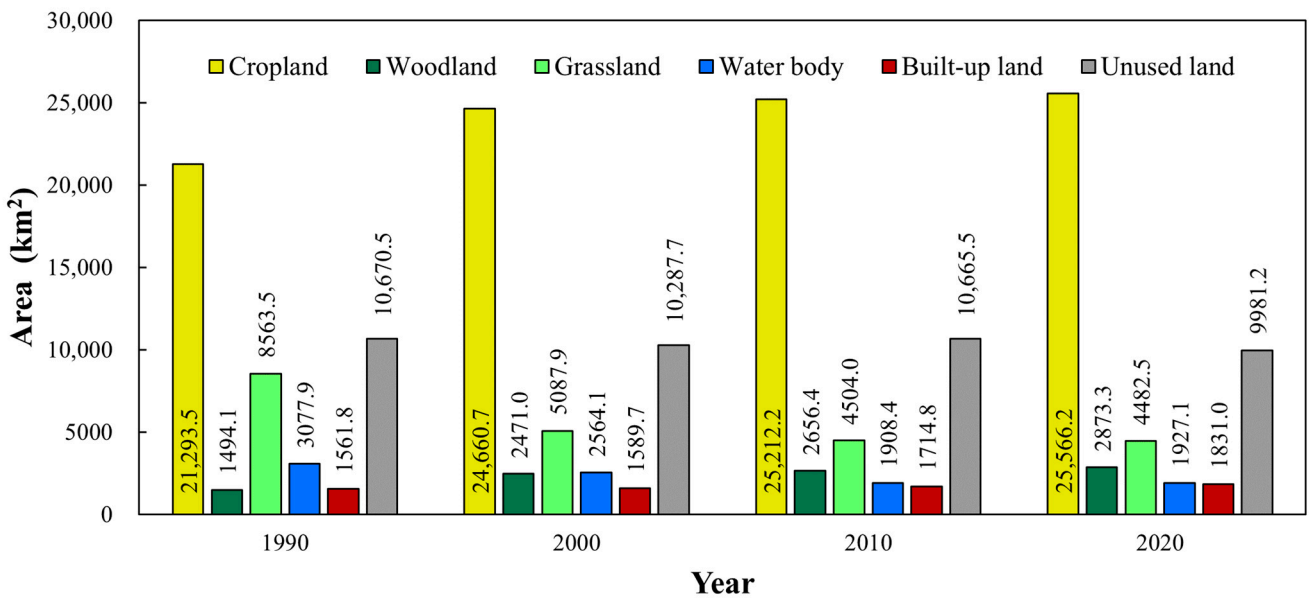
→ indicates the direction of land use transfer.

The interaction detector reflects the degree of influence of a factor by identifying the difference between the interaction of two factors and their individual effects. The impact of X_i and X_j is examined by comparing the q values of their interaction effect with the q values of their individual effects [44–46]. Furthermore, by evaluating the q_i and q_j of factors X_i and X_j respectively, the q_{ij} of the interaction of the two factors can be derived. Comparing q_i , q_j , and q_{ij} allow for the determination of the strength of the interaction effect.

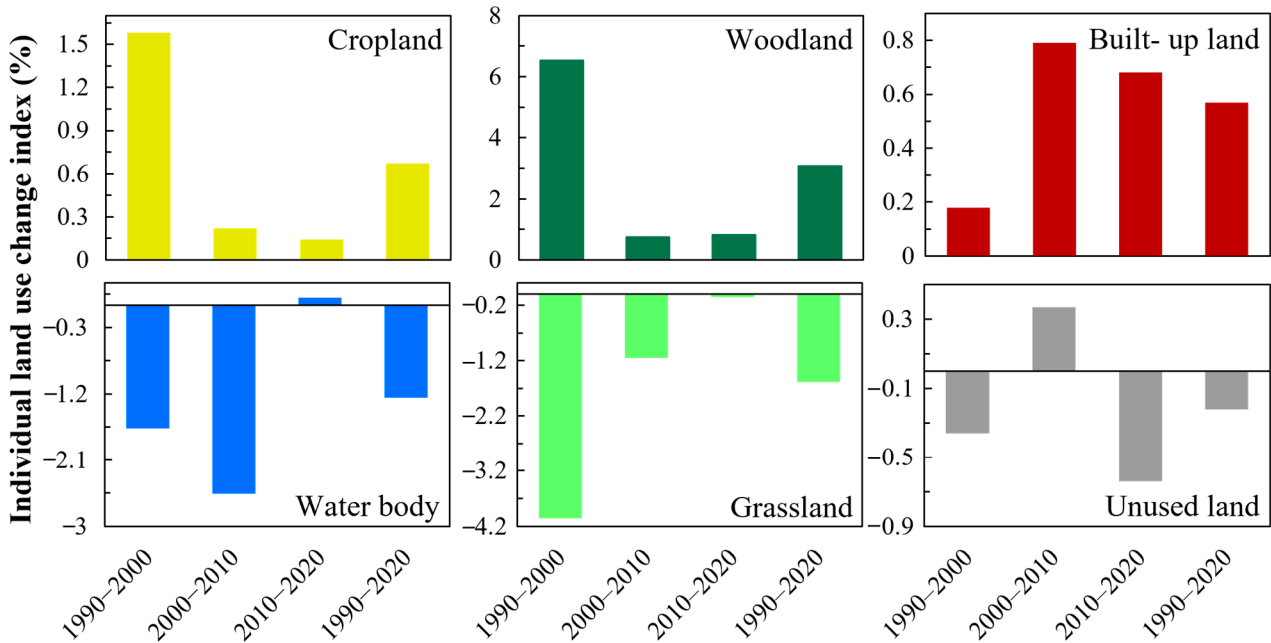
3. Results

3.1. Spatiotemporal Variation Analysis

Figure 2 compares the area and change index for six land-use types between 1990 and 2020. The comprehensive land-use change index in Western Jilin from 1990 to 2020 was 0.41%, with values of 0.85%, 0.72%, and 0.28% for the periods of 1990–2000, 2000–2010, and 2010–2020, respectively, indicating a decreasing trend in dynamics. As of 2020 (Figure 2a), the cropland area was 25,566.17 km² (54.79% of the total), while the woodland and grassland areas accounted for 2873.28 km² (6.16%) and 4482.5 km² (9.61%), respectively. The water body area accounted for 1927.05 km² (4.13%), and the built-up land area was 1831 km² (3.92%). The unused land accounted for 9981.2 km² (21.39%).



(a)



(b)

Figure 2. Changes in land-use types from 1990–2020. (a) Area. (b) Individual land use change index.

Cropland exhibited continuous expansion throughout the observed period (Figure 2b). From 1990 to 2020, the cropland area experienced a substantial increase of 4272.72 km², indicating a growth rate of 20%. The three-decade land-use change indices showed a downward trend, with values of 1.58%, 0.22%, and 0.15%.

Woodland demonstrated a gradual upward trend (Figure 2b). Between 1990 and 2020, the woodland area expanded by 1379.21 km², corresponding to a notable growth rate of 92.3%. The land-use change indices for the three decades were 6.54%, 0.75%, and 0.82%, indicating a stable growth pattern and a consistent increase.

Grassland experienced a significant reduction of 4080.96 km² (47.66%) as a large portion was converted to other land-use types between 1990 and 2000 (Figure 2b). However, the land-use change indices for the subsequent three decades demonstrated a gradual deceleration in the rate of decline, with values of −4.06%, −1.15%, and −0.05%, suggesting a transition towards a more stabilized and lessening decline from 2000.

The proportion of water bodies in the study area remained relatively stable, ranging between 4% and 7% (Figure 2b). However, from 1990 to 2020, there was a decrease in the area by 1150.88 km² (37.94%), with dynamics of −1.67%, −2.56%, and 0.1% observed for the three decades. Notably, there has been an upward trend in the water area since the year 2000.

The built-up land area exhibited a consistent and steady increase (Figure 2b). Spatially, the number of built-up land areas noticeably expanded, while existing built-up land areas continued to grow. Over the period from 1990 to 2020, the built-up land area increased by 269.21 km² (17.24%). The dynamics for the three decades were 0.18%, 0.79%, and 0.68%.

Unused land was a prominent land-use category in the study area, but its area steadily diminished over time (Figure 2b). Between 1990 and 2020, the unused land area decreased by 689.29 km² (6.46%). The dynamics for the three decades were −0.36%, 0.37%, and −0.64%. Notably, a certain amount of land was converted to unused land during the period from 2000 to 2010.

Figure 3 illustrates the spatial distribution of land use types from 1990 to 2020 in the study area. Cropland is the dominant land-use type, exhibiting a widespread distribution in both the eastern and western regions. The spatial pattern of cropland has remained relatively stable over time, suggesting a saturation of cropland utilization in the research area; Woodland, although occupying a relatively smaller area, has experienced some noteworthy changes. Between 1990 and 2000, a significant expansion of woodland occurred in the southern part of the study area. Furthermore, the central region has also shown a trend of woodland expansion from 1990 to the present. Grassland, predominantly distributed in the western and southern parts of the research area, has experienced a continuous decline in its extent since 1990. The most severe reduction has occurred in the western region, which is likely due to its proximity to Inner Mongolia, where factors such as wind, sand, and overgrazing have contributed to the persistent decrease in grassland.

The water bodies in the study area are mainly associated with the Songhua River and Liao River systems in the northern region, as well as various lakes distributed in the central and northern parts. Between 1990 and 2010, the water bodies in the southern region experienced a notable reduction, which was replaced by unused land. Additionally, the areas surrounding the water bodies and grasslands often contain a considerable amount of saline-alkali land. Due to the relatively low elevation in the central and southern parts of the study area, the accumulation of river water and surface runoff has led to the concentration of salts and alkali, which can both support grassland growth and cause extensive land salinization, resulting in the expansion of unused land. This interplay between water bodies, grasslands, and unused land is particularly evident between 2000 and 2010, when the significant reduction in water bodies and woodlands led to a substantial increase in unused land (Figure 2b). The built-up area has exhibited a stable and moderate expansion from 1990–2020 without any significant clustering. This suggests that the cities in Western Jilin will continue to develop in the future, which may contribute to a decrease in the area of unused land surrounding the urban centers.

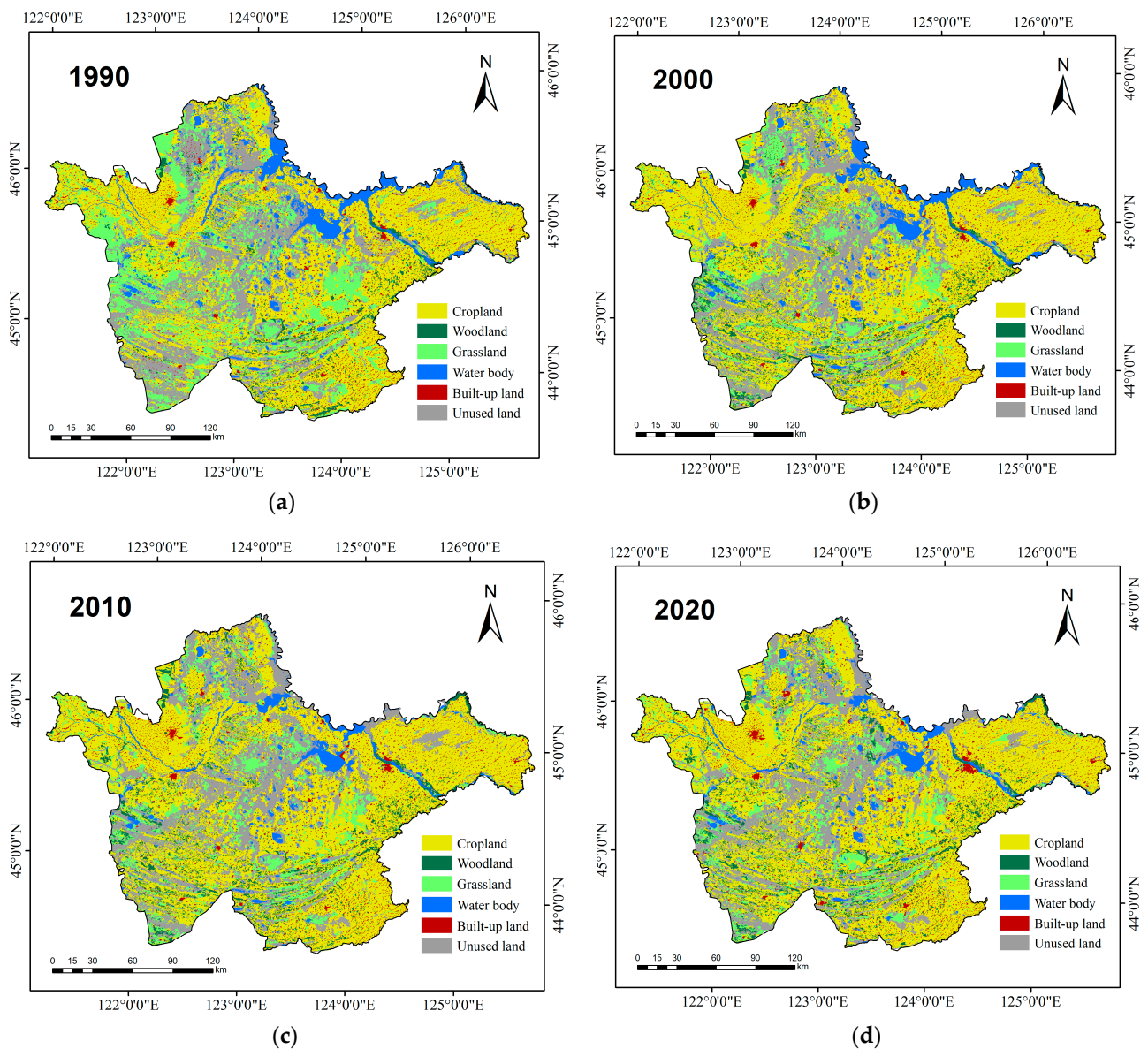


Figure 3. Spatial distribution of land use types from 1990–2020, (a) 1990; (b) 2000; (c) 2010; (d) 2020.

3.2. Type Conversion Characteristics

To provide a comprehensive analysis of land-use changes in the western ecological barrier zone of Jilin Province, we conducted a detailed examination of the trends (Figure 4), and the corresponding areas (Table 3). From 1990 to 2020, the predominant land-use conversions in the study area occurred among cropland, grassland, unused land, and water bodies. Specifically, a significant portion of cropland, amounting to 3378.73 km², underwent conversion to grassland, which accounted for 58.94% of the total cropland conversion area. Additionally, 1540.07 km² of cropland was transformed into unused land. Among the conversions from unused land, 2753.11 km² were converted to grassland, representing 46.94% of the total unused land conversion area. Furthermore, 1319.09 km² of water bodies experienced conversion, with 56.44% of them being transformed into unused land, indicating a fluctuating pattern of change.

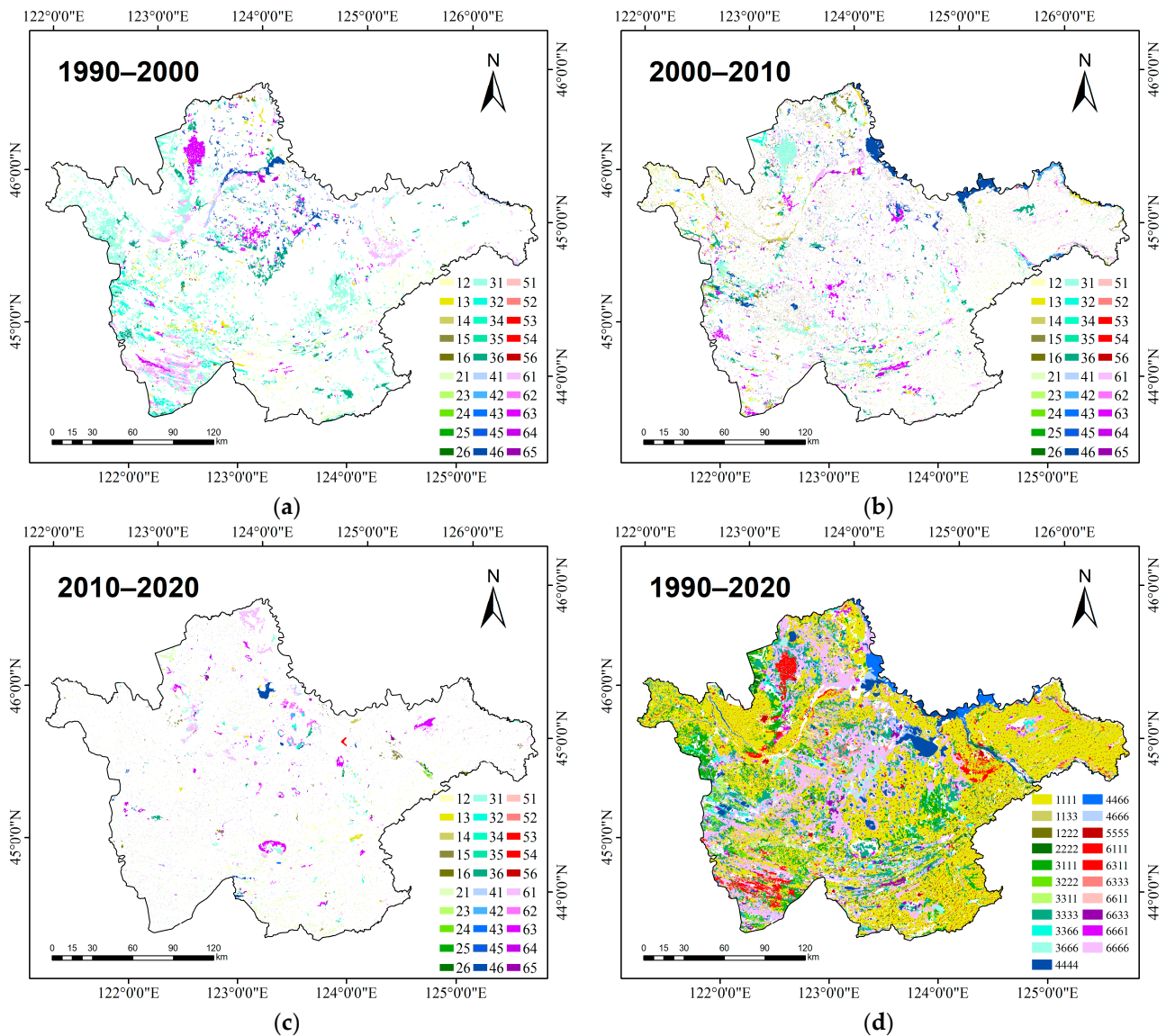


Figure 4. Spatial distribution of land-use change types from 1990–2020, (a) 1990–2000; (b) 2000–2010; (c) 2010–2020; (d) 1990–2020 (“12” represents conversion of cropland to woodland, “13” means cropland converted to grassland, “1111” means the area where cropland remains unchanged over 4 periods, “1133” means the area that was cropland in 1990, 2020, converted to grassland in 2010, 2020, and so on).

Distinct patterns of land-use changes emerged across the three periods: 1990–2000, 2000–2010, and 2010–2020 (Table 3). In the first period, the western region of the study area underwent significant increases in cropland, woodland, and unused land, accompanied by a loss of grassland. Specifically, 285.21 km² (19.09%) of woodland, 2920.88 km² (34.11%) of grassland, and 917.8 km² of unused land were changed to cropland. Conversely, 587.37 km² (2.76%) of cropland, 113.24 km² (1.06%) of grassland, and 588.02 km² (6.87%) of unused land were transitioned to woodland. Although 598.57 km² (5.61%) of unused land was converted to grassland, 777.15 km² (9.08%) of grassland still underwent conversion to unused land. Additionally, a significant loss of water bodies occurred, with 726.95 km² (28.35%) being altered to unused land, predominantly concentrated in the southern part of the study area.

Table 3. Land-use transfer change in Western Jilin (km²).

1990–2020	Cropland (1)	Woodland (2)	Grassland (3)	Water Body (4)	Built-Up Land (5)	Unused Land (6)	Sum
Cropland	20,401.7	587.37	194.17	9.71	22.64	77.86	891.75
Woodland	285.21	1181.81	20.85	0.88	1.46	3.86	312.26
Grassland	2920.88	588.02	4253.72	17.38	6.32	777.15	4309.74
Water body	131.76	0.3	20.44	2426.71	0.05	498.67	651.22
Built-up land	3.39	0.3	0.15	0.01	1557.74	0.2	4.04
Unused land	917.8	113.24	598.57	109.4	1.52	8929.98	1740.53
Sum	4259.04	1289.22	834.17	137.38	31.99	1357.75	-
2000–2010	Cropland	Woodland	Grassland	Water Body	Built-Up Land	Unused Land	Sum
Cropland	23,010.49	421.78	457.99	124.25	260.21	386.03	1650.25
Woodland	318.4	1956.86	104.77	20.94	15.05	55.02	514.18
Grassland	997.08	136.72	3229.79	13.56	27.37	683.37	1858.1
Water body	87.76	84.89	76.65	1572.54	15.32	726.95	991.56
Built-up land	205.38	11.71	14.31	1.73	1335.4	21.2	254.33
Unused land	593.12	44.49	620.46	175.34	61.4	8792.91	1494.81
Sum	2201.74	699.58	1274.18	335.82	379.34	1872.57	-
2010–2020	Cropland	Woodland	Grassland	Water Body	Built-Up Land	Unused Land	Sum
Cropland	24,513.91	373.51	78.98	26.12	133.64	86.07	698.32
Woodland	270.89	2337.64	8.98	17.08	4.25	17.61	318.8
Grassland	236.21	38.43	4120.12	26.44	13.12	69.64	383.85
Water body	22.74	11.39	8.42	1735.63	0.93	129.26	172.73
Built-up land	55.66	4.83	3.18	12.23	1632.72	6.12	82.03
Unused land	466.76	107.48	262.82	109.55	46.34	9672.52	992.95
Sum	1052.26	535.64	362.39	191.42	198.28	308.69	-

During the second period (2000–2010), the increase in cropland was primarily due to conversions from woodland and grassland, with 318.4 km² (12.89%) of woodland and 997.08 km² (19.6%) of grassland shifting to cropland (Table 3). Grassland and unused land experienced frequent exchanges, with 683.37 km² (13.43%) of grassland being converted to unused land and 620.46 km² (12.17%) of unused land undergoing conversion to grassland. Furthermore, the water bodies in the southern part of the study area suffered further loss, with 726.95 km² (28.35%) transitioning to unused land.

In the third period (2010–2020), the increase in cropland and unused land was minimal, while woodland and built-up land exhibited growth (Table 3). However, cropland remained the dominant land-use type with respect to conversions. Specifically, 270.89 km² (10.2%) of woodland and 466.76 km² (4.38%) of unused land were converted to cropland, while 129.26 km² (6.77%) of water bodies were lost and transformed into unused land, primarily concentrated in the central part of the study area.

In the study area of Western Jilin Province, the overall trend of land-use changes reflects some notable patterns (Table 3). The cropland area continued to expand, although at a gradually slowing rate. The most significant increase occurred from 1990 to 2000, with a substantial gain of approximately 3367.29 km². Conversely, the grassland area exhibited the most substantial decrease, although the rate of decline gradually decelerated. The largest reduction occurred during 1990–2000, resulting in a total loss of 3475.58 km². This consistent conversion of grassland to cropland suggests a significant conversion of approximately 2920.88 km² of grassland to cropland during that decade; Woodland and built-up land exhibited steady upward trends, albeit with smaller areas in the study area. Water bodies initially experienced a decline, followed by a slight increase. From 1990 to 2010, water bodies continuously decreased, but a slight upward trend was observed from 2010 to 2020. These changes likely reflect land development or water management projects implemented during this period. Water bodies, along with unused land, including saline-alkali land, have been engaged in a persistent tug-of-war, representing a vulnerable ecosystem component. In this study, the water body area in Western Jilin Province has been affected, experiencing a truncation, but it has shown signs of gradual recovery and expansion.

Furthermore, the conversion of land-use types is primarily characterized by the long-term stability and persistence of cropland and unused land, mainly concentrated in the fertile black soil areas in the eastern part of the study area and around rivers and lakes (Figure 4). The degradation of grassland into cropland and unused land occurred predom-

inantly during the middle period of the study (2000–2010), while the area occupied by land-use types undergoing repeated changes was minimal, representing less than 1% of the total. These findings indicate that land-use conversion in the study area is relatively limited and mainly involves mutual transformations between cropland, grassland, unused land, and water bodies. These land-use conversion activities may reflect the influence of policy implementation, urbanization, agricultural land development, and infrastructure construction on land-use dynamics.

3.3. Topographic-Climatic-Economic Factors

3.3.1. Factor Detection

The factor detection results indicate that the influence of various factors on land-use change varies significantly across different land-use types (Figure 5). The main influencing factors for cropland-to-woodland conversion are agricultural population (X10), livestock population (X11), and urbanization level (X12), with q -values of 0.25, 0.14, and 0.12, respectively. The greater the agricultural population and livestock, the greater the demand for rural cropland. However, the higher the urbanization level, the lower the demand for cropland. The main influencing factors for cropland-to-grassland conversion are agricultural population (X10), livestock population (X11), and soil moisture content (X6), with q -values of 0.11, 0.05, and 0.03, respectively. It can be seen that in addition to X10 and X11, the restoration of grassland is also constrained by soil moisture content (X6). The main influencing factors for cropland-to-built-up land conversion are also agricultural population (X10), livestock population (X11), and urbanization level (X12), with q -values of 0.35, 0.14, and 0.11, respectively. That is, the lower the agricultural population and livestock, and the higher the urbanization level, the more likely cropland is to be converted to built-up land. The dominant factor for woodland-to-cropland and woodland-to-built-up land conversions is the agricultural population (X10), and the larger the agricultural population, the greater the demand for farmers to reclaim woodland and build houses. The influencing factors for woodland-to-grassland conversion are more numerous and relatively equal in effect, with the top six being slope (X2), elevation (X1), aspect (X3), aridity index (X7), temperature (X5), and soil moisture content (X6), with q -values of 0.070, 0.053, 0.047, 0.043, 0.042, and 0.038, respectively. It can be said that the conversion of woodland to grassland is mainly influenced by climatic and topographic conditions.

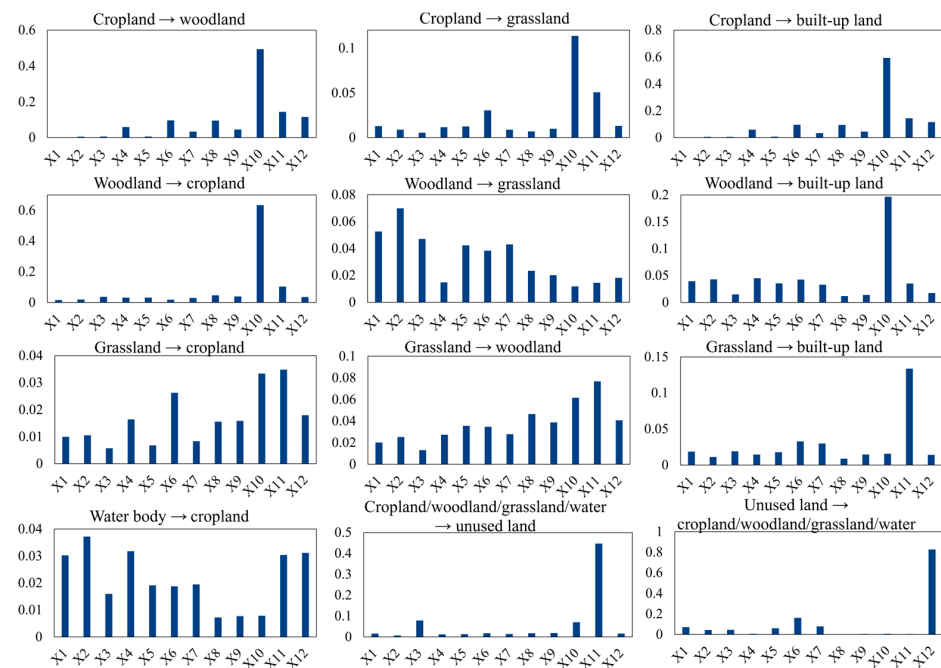


Figure 5. Explanatory power (q) of driving factors from 1990 to 2020.

Under suitable soil moisture conditions (X6), the larger the agricultural population (X10) and livestock population (X11), the more likely grassland is to be converted to cropland. The main influencing factors for grassland-to-woodland conversion are livestock population (X11), agricultural population (X10), GDP (X8), and urbanization level (X12), with q-values of 0.077, 0.062, 0.047, and 0.041, respectively. As GDP and urbanization levels rise, the agricultural population urbanization process accelerates, reducing the demand for livestock on grassland, which is conducive to the conversion of grassland to woodland. The livestock population (X11) has a relatively prominent impact on the conversion of grassland to built-up land, with a q-value of 0.134, mainly because rural grassland can be used for livestock grazing, and if the livestock population decreases, grassland is more likely to be occupied by built-up land. The influencing factors for water body-to-cropland conversion are relatively complex, with slope (X2), precipitation (X4), urbanization level (X12), elevation (X1), and livestock population (X11) having a relatively large impact, with q-values of 0.037, 0.032, 0.031, 0.030, and 0.030, respectively. On the one hand, the conversion of water bodies to cropland has clear requirements for topographic and climatic conditions, and the probability of this conversion increases when the slope is low, the elevation is low, and the precipitation decreases. On the other hand, as the urbanization level rises and the number of livestock owned by farmers decreases, the demand for using water bodies for washing and livestock drinking decreases, and the probability of water bodies being converted to cropland also increases. The main influencing factor for the conversion of cropland, woodland, grassland, and water bodies to unused land is also the livestock population (X11). The logic is similar to that of water bodies being converted to cropland—when the livestock population decreases, the availability of cropland, woodland, grassland, and water bodies to a certain extent becomes “discounted”, and their utilization rate decreases, leading to their conversion to unused land. The conversion of unused land to cropland, woodland, grassland, and water bodies is mainly influenced by the urbanization level (X12), and as the urbanization process progresses, unused land is constantly converted to other land-use types, reflecting the full and reasonable utilization of land resources.

3.3.2. Interaction Detection

The interactive detection of land-use change driving factors (Figure 6) indicates that the influence of the interactions between different factors is more significant. In the process of cropland conversion to woodland, the interaction between agricultural population (X10) and urbanization level (X12) significantly enhances their influence, while the interaction between livestock number (X11) and precipitation (X4), while GDP (X8) also strengthens their impact. During the cropland-to-grassland transition, the interaction between soil moisture (X6) and temperature (X5) is more favorable for the development of grassland. For cropland conversion to built-up land, the influence of agricultural population (X10) and livestock number (X11) is further enhanced when they interact with precipitation (X4) and GDP (X8), respectively. The dominant factor for woodland-to-cropland conversion is agricultural population (X10), whose effect acts relatively independently, while climate (X5) and the aridity index (X7) may actually be more conducive to promoting the transformation of woodland to cropland when they interact. The most prominent interactive force in the woodland-to-grassland process is elevation (X1) and slope (X2), indicating that the development of grassland has higher requirements for topographic conditions. The dominant factor for woodland conversion to built-up land is also the agricultural population (X10), and its speed of transformation is accelerated when interacting with GDP (X8) as an influencing factor.

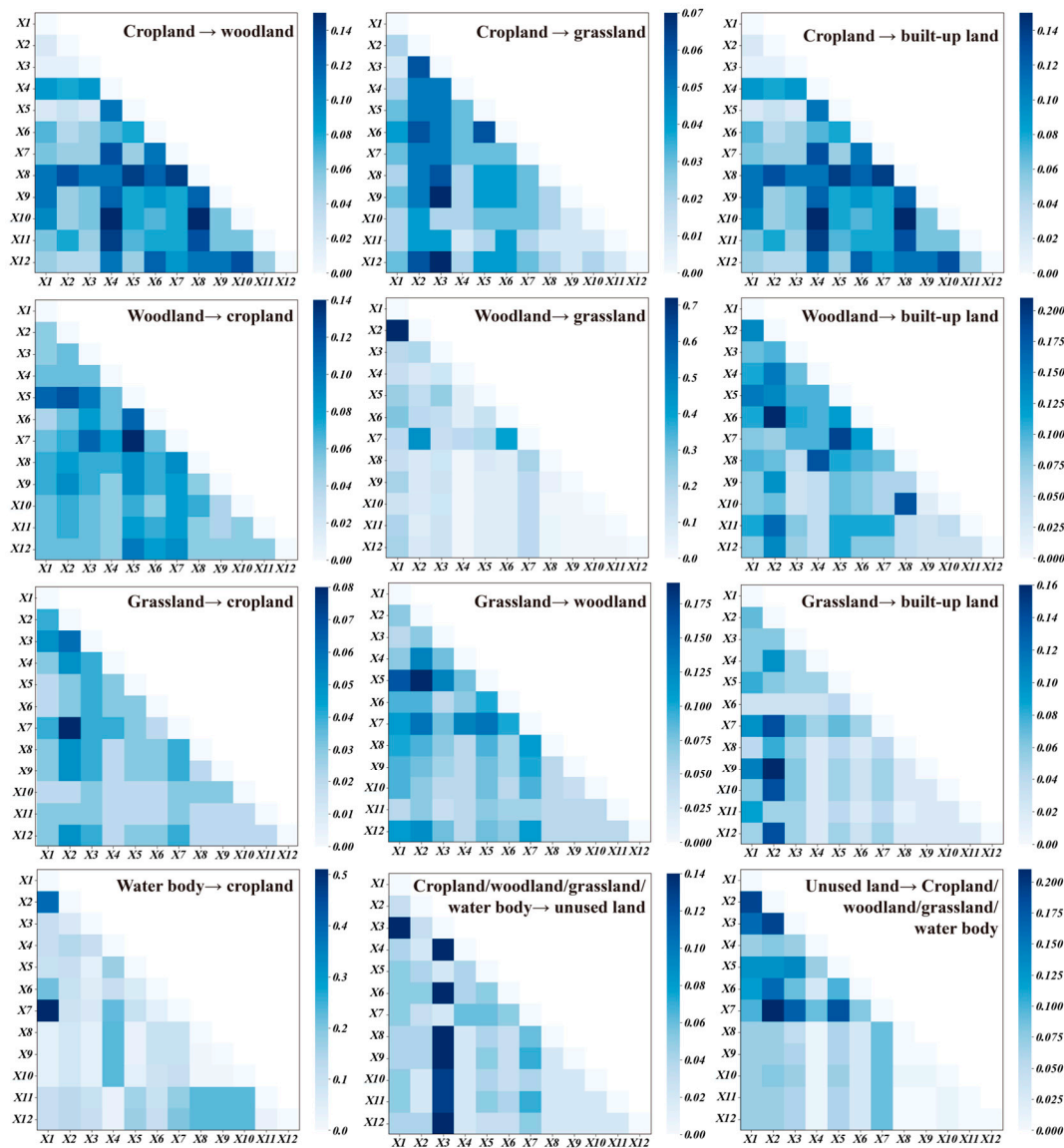


Figure 6. Results of interaction of 1990–2020, color scale: the value of (q) .

In the grassland-to-cropland process, the interaction between slope (X2) and the aridity index (X7) is relatively obvious. When slope (X2) interacts with temperature (X5), i.e., suitable slope and temperature, grassland is more likely to be converted to woodland. The main driver of grassland conversion to built-up land is livestock number (X11), and the only factor that has a certain influence according to the interactive detection is elevation (X1). The most prominent interactive effect in the water body-to-cropland transition is between the drought index (X7) and elevation (X1). In the processes of cropland, woodland, grassland, and water body transitioning to unused land, the influence of most factors other than slope aspect (X3), temperature (X5), and the aridity index (X7) are significantly enhanced when interacting with slope aspect. When unused land transitions to cropland, woodland, grassland, water body, and unused land, urbanization level (X12) is the dominant factor, its driving force will be amplified when interacting with the drought index (X7).

3.3.3. Risk Detection

The spatial distribution pattern of land-use changes in the study area from 1990–2020 was influenced by a variety of factors, including topography, climate, and economy, rather than being an isolated phenomenon. There is a close relationship between natural and

human systems. We further examined the impacts of different driving factors on various land-use change patterns and summarized the results in Tables 4 and 5. Overall, the ranges of driving factors for different types of land-use conversion show distinct differences. Natural conditions play a dominant role in the transition from “natural vegetation” to “artificial use”, while socioeconomic factors play an important role in the transitions among “artificial use” types.

Table 4. Adaptation ranges suitable for topographic and climatic covariates to land-use changes.

Type	DEM (m)	Slope (°)	Aspect (°)	Annual Rainfall (mm)	Average Annual Temperature (°)	Soil Moisture (cm ³ /cm ³)	Aridity Index
Cropland → woodland	170–190	36.5–39.5	124–165	14.1–15.3	6.36–6.49	0.230–0.235	0.305–0.326
Cropland → grassland	303–361	33.9–37.8	170–176	14.1–15.8	6.17–6.42	0.215–0.232	0.292–0.315
Cropland → built-up land	145–156	16.5–32	151–169	18.1–20.9	6.19–6.67	0.256–0.286	0.229–0.310
Woodland → cropland	208–243	42.4–50.2	203–230	17.8–20.9	5.43–5.49	0.230–0.236	0.340–0.361
Woodland → grassland	159–165	41.9–45.7	167–180	16.3–17.2	6.15–6.26	0.236–0.239	0.355–0.367
Woodland → built-up land	159–173	62.2–76.5	202–230	17.5–20.9	5.43–5.50	0.222–0.230	0.321–0.348
Grassland → cropland	304–362	35.8–39.7	182–196	14.1–15.2	6.00–6.24	0.250–0.268	0.360–0.348
Grassland → woodland	160–167	35.8–39.1	142–155	16.3–17.0	6.61–6.67	0.220–0.229	0.292–0.298
Grassland → built-up land	146–155	16.9–26.7	164–168	14.1–16.2	5.89–6.05	0.219–0.241	0.333–0.351
Water body → cropland	159–173	62.2–76.5	202–230	17.8–18.1	5.43–5.50	0.222–0.230	0.321–0.348
Cropland/woodland/grassland/water → unused land	128–142	70.4–80.9	66.8–83.8	17.0–17.2	5.93–6.06	0.213–0.227	0.343–0.361
Unused land → cropland/woodland/grassland/water	167–186	20.5–32.4	167–171	14.1–15.3	6.30–6.46	0.202–0.221	0.338–0.352

Table 5. Adaptation ranges suitable for economic covariates to land-use change.

Type	GDP (in 10,000 s RMB)	Population Size (in 10,000 s)	Agricultural Population Size (in 10,000 s)	Livestock (Head)	Urbanization Level (%)
Cropland → woodland	777,000–1,170,000	35.3–52.2	11.6–13.2	35,800–54,500	43.4–77.3
Cropland → grassland	665,000–777,000	29.8–35.3	8.02–12.4	25,500–43,100	63.7–67.2
Cropland → built-up land	1,440,000–2,240,000	43.8–51.2	28.8–43.4	15,100–25,500	33.1–45.2
Woodland → cropland	1,400,000–1,420,000	57.2–63.0	12.4–19.0	72,600–123,000	24.2–36.1
Woodland → grassland	1,400,000–1,420,000	57.2–63.0	30.4–43.4	56,400–83,200	24.2–36.1
Woodland → built-up land	777,000–909,000	43.3–71.0	28.8–43.4	46,400–56,400	45.2–61.5
Grassland → cropland	665,000–777,000	27.1–35.3	8.02–12.4	25,500–43,100	63.7–67.2
Grassland → woodland	665,000–777,000	26.3–35.3	8.02–12.4	25,500–43,100	67.2–70.4
Grassland → built-up land	655,000–777,000	27.1–35.3	10.6–11.6	25,500–43,100	63.7–67.2
Water body → cropland	777,000–909,000	26.3–27.1	19.0–28.8	46,400–56,400	45.2–61.5
Cropland/woodland/grassland/water → unused land	901,000–1,220,000	35.3–37.8	19.0–28.8	15,100–25,500	45.2–61.5
Unused land → cropland/woodland/grassland/water	777,000–1,310,000	35.3–49.0	11.6–13.9	35,800–54,500	43.4–77.3

For example, the conversion from cropland to woodland and grassland requires higher elevations, while the conversion from cropland to built-up land mainly occurs in areas with lower elevations and slopes. This suggests that regions with higher elevations and steeper slopes are more suitable for the conversion of cropland to natural vegetation, while flat areas are more suitable for urban construction. Similarly, different types of conversions have distinct suitable climate conditions, with built-up land conversion requiring relatively lower water conditions. Key socioeconomic factors such as GDP, population size, agricultural population size, livestock, and urbanization level are also crucial drivers. Different conversion types have large variations in their suitable ranges for these factors; for instance, a higher GDP level is favorable for the conversion from cropland or woodland to built-up land, while a lower GDP level is more suitable for the conversion from woodland or grassland to cropland.

These driving factors present complex suitable ranges across different land use conversion types, reflecting the multidimensional characteristics of land use changes. In the future, comprehensive consideration of natural environmental and socioeconomic conditions is needed to develop differentiated land-use policies and management measures for specific regions. However, it should be noted that different land-use conversion pathways require different combinations of driving factors, and these driving factors also interact with each

other, such as the synergistic changes in temperature and precipitation patterns, and the urbanization process leading to population growth and economic development.

3.4. Policy Factors

In addition to the influences of topographic, climatic, and economic factors, policy elements also play a crucial driving role in land-use type transitions. Table 6 provides the policies and regulations that have been in effect from 1990 to 2020 within the research area.

Table 6. Key policies and statutes related to western Jilin from 1990 to 2020.

Time	Main Policy	Type	Trend	Direction	Rate (%)
Before 1990	Three North Shelter Forest Program (1978–2050) [47]	-	-	-	-
1990–2000	Water Conservancy Project during 8th Five-Year Plan Period (1991–1995) [48]	Cropland	↑	Woodland	1.58
	Returning of Farmland to River (Lake) Program (1993–2016) [49]	Woodland	↑	Cropland, Grassland	6.54
		Grassland	↓	Woodland, Cropland	−4.06
	The Outline of National Demonstration Zone Construction Planning (1996–2050) [50]	Water body	↓	Unused land	−1.67
	Natural Forest Protection Program (1998–2020) [51]	Built-up land	↑	Cropland, Woodland	0.18
Sloping Land Conversion Program (1999–2019) [52,53]	Unused land	↓	Cropland, Woodland	−0.36	
2000–2010	National Wildlife Protection and Nature Reserve Construction Program (2001–2050) [54]	Cropland	↑	Woodland	0.22
		Woodland	↑	Cropland	0.75
	Alkali Control Project in the West of Jilin Province (2002–) [28]	Grassland	↓	Woodland, Cropland	−1.15
	Conversion of Farmland to Grassland Program (2003–2008) [55]	Water body	↓	Unused land	−2.56
	Wetland Protection Program (2002–2030) [56]	Built-up land	↑	Unused land	0.79
The Major Land Consolidation Project in the West of Jilin Province (2008–) [28]	Unused land	↑	Water body	0.37	
2010–2020	National Desertification Prevention and Control Plan (2010–2020) [58]	Cropland	↑	Woodland, Grassland	0.14
		Woodland	↑	Cropland, Grassland	0.82
	Nationwide Major Function Oriented Zoning (2011–2021) [59]	Grassland	↓	Woodland, Water body	−0.05
	Development Goals of “Three-life space” (2012–) [60]	Water body	↑	Unused land	0.1
	River-lake Connection Project (2013–) [61]	Built-up land	↑	Cropland	0.68
Management Measures for Ecological Protection Guidelines for the Red Line of Ecological Protection (2016–) [58]	Unused land	↓	Water body	−0.64	
Wetland Protection and Restoration System Plan (2017–) [56]					
After 2020	The Master Plan for Major Projects of National Important Ecosystem Protection and Restoration (2021–2035) [62]	-	-	-	-
	Land Spatial Ecological Restoration Planning (2021–2035) [63]				

↑ represents an increase in the area of land-use types, while ↓ represents a decrease.

From 1990 to 2000, the movement of the rural–urban population was still constrained by agricultural taxes, resulting in high demand from farmers for cropland and land development, leading to a significant increase in cropland area. The conversion of woodland, grassland, and unused land into cropland increased agricultural production. However, a noteworthy change during this period was the substantial growth of woodland, which created a tug-of-war situation with land cultivation. This growth was primarily attributed to the implementation of forest land protection plans such as the “Three-North Shelter Forest Program (1978–2050)”, “Natural Forest Protection Project (1998–2020)”, “Sloping Land Conversion Program (1999–2019)”, and “Natural Forest Protection Program (1998–2020)”. The policy support provided by the “Outline of National Demonstration Zone Construction Planning (1996–2050)” also contributed to woodland protection. Furthermore, these policies drove significant reductions in grassland and unused land, with a large proportion converted to woodland.

From 2000 to 2010, in addition to the forest land-protection policies implemented from 1990–2000, the implementation of the “National Wildlife Protection and Nature Reserve Construction Program (2001–2050)” organized by the State Forestry Administration and the “Conversion of Farmland to Grassland Program (2003–2008)” resulted in a continued transformation of cropland into woodland and grassland, although at a slower pace in reducing grassland area. In 2006, the abolition of agricultural taxes coincided with a surge in urbanization accelerated during this period, leading to an increase in built-up land area.

“Wetland Protection Program (2003–2030)” also facilitated the large-scale conversion of unused land into water bodies.

From 2010 to 2020, the “River–Lake Connection project” launched in Baicheng City, Jilin Province in 2013, and the issuance of the “Wetland Protection and Restoration System Plan” by the State Council in 2017 resulted in a slower rate of conversion from water bodies to unused land, with the total area starting to increase. Continued implementation of policies and plans for natural forest protection, along with the official release of the “Nationwide Major Function Oriented Zoning” in 2011 and the “Management Measures for Jilin Province’s Ecological Protection Red Line Area (Trial)”, as notified by the Jilin Provincial People’s Government, further promoted the transformation from cropland to woodland and grassland. These measures ensured the continuous growth of forest land area and reduced the loss of grassland area. Since the 18th National Congress of the Communist Party of China in 2012, there has been an emphasis on adjusting the spatial structure to promote intensive and efficient production space, livable living space, and beautiful ecological space. In 2013 and 2014, further emphasis and adjustments were made to the “Three-life Space” concept, providing policy support for rural land consolidation and integration, which was the main reason for the reclamation of built-up land into cropland during this period. Meanwhile, the “100 Billion Cattles Grain Production Capacity Project (2009–2020)” ensured the continuous increase in cropland area.

The policies have a significant and rapid impact on land-use-type transitions. They can continue to exert influence during the effective period of implementation. Of course, if similar policies were implemented within the same period, the effects produced would be more considerable. Additionally, compared to national-level policy planning, local policies are more targeted and can assist in national policies and provide more rapid planning, guidance, and control of specific land-use patterns.

4. Discussion

Based on the analysis above, the land-use types in the study area have undergone significant changes under the influence of multiple factors, including the natural environment, social development, and policy regulations.

Cropland is the dominant land-use type, with an increase of 4272.72 km² from 1990 to 2020, primarily converted from grassland, unused land, and woodland. According to the factor detection results, the main driving factors for the conversion of grassland and woodland to cropland are agricultural population size, rainfall, and GDP. The interaction analysis further reveals that slope and aspect have a stronger influence on the conversion of unused land to cropland when interacting with temperature, rainfall, GDP, and population size. The increase in cropland is mainly driven by social development, as a larger agricultural population leads to a higher demand for reclamation. However, the conversion of woodland, grassland, and unused land to cropland is still constrained by natural environment and climate conditions.

The woodland area has increased significantly by 92.3% from 1990 to 2020, primarily converted from grassland, cropland, and unused land. The factor detection shows that the main driving factors for the conversion of grassland to woodland are DEM, the conversion of cropland to woodland is GDP, agricultural population size, and rain, and the conversion of unused land to woodland is slope, aspect, temperature, and population size. The results suggest that a single or a few driving factors are insufficient to explain the substantial increase in woodland area. The dynamic change rates of woodland were 6.54%, 0.75%, and 0.82% from 1990–2000, 2000–2010, and 2010–2020, respectively. The significant increase in woodland area was mainly driven by policy interventions, such as the “Returning of Farmland to River (Lake) Program (1993–2016)” [49], and the “Natural Forest Protection Program (1998–2020)” [51].

The grassland area has continuously decreased, with a decline rate of 47.66% from 1990 to 2000, mainly converted to cropland, unused land, and woodland. The factor detection shows that the main driving factors for the conversion of cropland to grassland are aspect,

GDP, rainfall, and agricultural population size, the conversion of unused land to grassland is slope, aspect, temperature, and population size, and the conversion of woodland-to-grassland is rainfall. The interaction analysis suggests that the decrease in grassland area is the result of both climate change and social development. It is worth noting that the dynamic change rate of grassland area decreased from -4.06% from 1990–2000 to -1.15% from 2000–2010, indicating the important impact of the “Conversion of Farmland to Grassland Program” [55] program implemented in 2003.

The water body area has decreased by 37.94%, mainly converted to unused land and cropland. The factor detection shows that the main driving factor for the conversion of the water body to cropland is DEM. The interaction analysis further reveals that DEM has a stronger influence when interacting with other drivers, and its impact is higher when interacting with natural factors than social factors. The decrease in water body area is primarily driven by changes in natural conditions. The dynamic change rates of water body area were -1.67% , -2.56% , and 0.1% in the three 10-year periods from 1990 to 2020, indicating that the “River–Lake Connection Project” [61] and “Wetland Protection and Restoration System Plan” [56] implemented since 2013 have effectively controlled the significant decrease in water body area.

The built-up land area has maintained an increasing trend, with a 17.24% increase from 1990 to 2020, mainly converted from cropland, unused land, and grassland. The factor detection shows that the main driving factors for the conversion of cropland to built-up land are GDP, population size, and urbanization level, and the conversion of grassland to built-up land are GDP, rainfall, and agricultural population size. The increase in built-up land area is the result of the advancement of urbanization, as higher GDP levels require more built-up land during the current stage of urbanization. From 1990 to 2000, the rapid urbanization process in China occupied a large amount of built-up land. However, after the implementation of the “pothook policy of urban construction land increase and rural residential land decrease” in 2000 [64], the speed of built-up land increase has slowed down under the concept of intensive and efficient land use.

The unused land has continuously decreased by 689.29 km² from 1990 to 2020, converted to cropland, grassland, woodland, and the water body. The factor detection shows that the main driving factors for the conversion of unused land to cropland, woodland, and grassland are slope, aspect, temperature, and population size. The decrease in unused land area is constrained by natural factors and requires human intervention. The targeted policy implementation, such as the “Alkali Control Project in the West of Jilin Province” in 2002 [28], has produced positive effects, as indicated by the dynamic change rates of -0.36% , 0.37% , and -0.64% in the three 10-year periods.

The conversion and driving mechanisms of different land-use types in the study area vary, requiring targeted efforts to cherish and reasonably utilize the land resources. Under the constraints of natural factors and the influence of economic development, policy interventions have more immediate effects. Therefore, rational policy formulation and implementation to plan land-use behaviors are crucial for ensuring ecological security and improving land-use efficiency. The sustainable utilization of land resources is a common issue facing the world. China’s land-use situations and problem-solving measures during the rapid urbanization phase from 1990 to 2020 may provide valuable references for other countries that need to continue promoting urbanization.

It is important to note that while this study employed quantitative analysis methods such as land change index and transition matrix to examine land-use change, these methods may introduce subjectivity and uncertainty. Additionally, due to data availability and accuracy constraints, the study covered the period from 1990 to 2020, which may not capture longer-term trends in land use change. Secondly, while 12 quantifiable topographic, climatic, and anthropogenic factors were considered, as well as qualitative analysis of policies, additional factors such as social and cultural factors may also influence land-use change. Therefore, several suggestions emerge for further research. Firstly, expanding the time range of the study, reducing the time intervals, and incorporating predictive results [11]

can capture longer-term, more detailed, and comprehensive trends in land-use change. Secondly, further exploration of other potential factors influencing land-use change, such as cultural factors and quantitative analysis of policy factors is recommended. Alternatively, with access to long-term time series land-use data, structural equation model (SEM) [65] and Granger causality methods [66,67] can be employed to uncover the genuine driving factors behind changes in land use. Additionally, employing more sophisticated spatial analysis methods to investigate local variations and heterogeneity in land-use change, such as spatial autocorrelation analysis (Moran's I, Geary's C [68,69]) to identify spatial clustering, dispersion, or randomness of land-use change patterns and detect hotspots, and spatial regression analysis (spatial lag models, spatial error models [70,71]) to explore the relationships between land-use variables and other spatial factors, would enhance the understanding of the driving factors of land-use change and determine the spatial impacts of different factors on land use.

5. Conclusions

As one of the ecological barrier transition zones, agro-pastoral transitional zones, and border areas, land-use change in Western Jilin is important for regional sustainable development, food security, macroeconomic regulation of land resources, and economic development. Therefore, it is necessary to analyze the spatiotemporal patterns of land-use change in Western Jilin through multiple periods to understand the underlying mechanisms and potential impacts. The research indicates: (1) The conversion of land-use types in Western Jilin is relatively limited and mainly involves exchanges between cropland, grassland, unused land, and water bodies. Cropland area has been increasing, but at a slower rate, with improved utilization, occupying a dominant position in land use in Western Jilin. Woodland and built-up land have steadily increased in area. Water bodies and grasslands have shown continuous recovery and are exhibiting a growth trend in the future. The trends demonstrate the consistency between land-use planning and the sustainable development strategy in Western Jilin, meeting the requirements for economic growth. (2) The factors influencing land-use change vary according to land-use types. Furthermore, there are correlations among the influencing factors, and the impact of dual (multiple) factors on land-use change is more significant than that of individual factors, exhibiting a trend of enhanced or nonlinear effects. (3) The influences of topographic-climatic and anthropogenic factors on land use are profound, long-term, and gradual; the impacts of policy factors show rapid and drastic effects in the short term. For instance, the decrease in water area was influenced by natural conditions. However, since 2013, the "river-lake connectivity project" and wetland conservation plans have effectively controlled the significant reduction in water area.

Conducting a multi-period analysis of land-use change can reflect the impacts of natural and human activities on land resources, which serve as the foundation for human survival and development. In the future, further exploration of other research methods, such as quantitative assessment of policy factors on land-use change in Western Jilin, is recommended. This quantitative assessment aims to evaluate the effects of the combined natural-policy factors on land-use-type transitions, thereby promoting the construction of an ecological civilization in the ecological barrier transition zone and facilitating the healthy development of the regional economy.

Author Contributions: Conceptualization, S.W. and Y.W.; data curation, S.W., T.T., B.L. and M.A.B.; formal analysis, S.W. and C.S.; funding acquisition, Y.W.; investigation, S.W., T.T. and Y.W.; methodology, S.W. and Y.W.; resources, S.W. and M.A.B.; software, S.W. and M.A.B.; supervision, Y.W.; validation, S.W. and Y.W.; visualization, S.W.; writing—original draft, S.W., C.S. and M.A.B.; writing—review and editing, S.W., Y.W. and Y.M. All authors have read and agreed to the published version of the manuscript.

Funding: This research was supported by the Key Project of the National Natural Science Foundation of China (42230810), the National Key Research and Development Program of China (2021YFC2901801),

the National Social Science Fund of China (18ZDA166), and the Jilin University Research Fund (45123031F025).

Data Availability Statement: The data presented in this study are available upon request from the corresponding author. The data are not publicly available due to privacy.

Acknowledgments: We would like to thank the anonymous referee for his/her helpful comments that improved the manuscript. The authors are grateful for the support of the staff at the 601 Laboratory, College of Geo-exploration Science and Technology, Jilin University, for their assistance in the completion of the experiments.

Conflicts of Interest: The authors declare no conflicts of interest.

References

- Colglazier, W. Sustainable development agenda: 2030. *Science* **2015**, *349*, 1048–1050. [[CrossRef](#)] [[PubMed](#)]
- Brito, L. Analyzing Sustainable Development Goals. *Science* **2012**, *336*, 1396. [[CrossRef](#)] [[PubMed](#)]
- Fan, J. Draft of major function oriented zoning of China. *Acta Geogr. Sin.* **2015**, *70*, 186–201. (In Chinese) [[CrossRef](#)]
- Fu, B. Several key points in territorial ecological restoration. *Bull. Chin. Acad. Sci.* **2021**, *36*, 64–69. (In Chinese) [[CrossRef](#)]
- Su, Y.-Z.; Zhao, H.-L.; Zhang, T.-H.; Zhao, X.-Y. Soil properties following cultivation and non-grazing of a semi-arid sandy grassland in northern China. *Soil Tillage Res.* **2004**, *75*, 27–36. [[CrossRef](#)]
- Piao, S.L.; Liu, Q.; Chen, A.P.; Janssens, I.A.; Fu, Y.S.; Dai, J.H.; Liu, L.L.; Lian, X.; Shen, M.G.; Zhu, X.L. Plant phenology and global climate change: Current progresses and challenges. *Glob. Chang. Biol.* **2019**, *25*, 1922–1940. [[CrossRef](#)] [[PubMed](#)]
- Wairiu, M. Land degradation and sustainable land management practices in Pacific Island Countries. *Reg. Environ. Chang.* **2017**, *17*, 1053–1064. [[CrossRef](#)]
- Wang, X.; LESL, M.; Zhang, M. Ecosystem pattern change and its influencing factors of “two barriers and three belts”. *Chin. J. Ecol.* **2019**, *38*, 2138–2148. (In Chinese) [[CrossRef](#)]
- Fei, L.; Shuwen, Z.; Jiuchun, Y.; Liping, C.; Haijuan, Y.; Kun, B. Effects of land use change on ecosystem services value in West Jilin since the reform and opening of China. *Ecosyst. Serv.* **2018**, *31*, 12–20. [[CrossRef](#)]
- Li, C.; Wu, Y.M.; Gao, B.P.; Zheng, K.J.; Wu, Y.; Li, C. Multi-scenario simulation of ecosystem service value for optimization of land use in the Sichuan-Yunnan ecological barrier, China. *Ecol. Indic.* **2021**, *132*, 108328. [[CrossRef](#)]
- Wen, S.; Wang, Y.; Song, H.; Liu, H.; Sun, Z.; Bilal, M.A. Integrated Predictive Modeling and Policy Factor Analysis for the Land Use Dynamics of the Western Jilin. *Atmosphere* **2024**, *15*, 288. [[CrossRef](#)]
- Li, Y.; Luo, Y.; Gang, L.; Ouyang, Z.; Zheng, H. Effects of land use change on ecosystem services: A case study in Miyun reservoir watershed. *Acta Ecol. Sin.* **2013**, *33*, 726–736.
- Qiu, J. China: The third pole. *Nature* **2008**, *454*, 393–396. [[CrossRef](#)] [[PubMed](#)]
- Kang, S.; Xu, Y.; You, Q.; Flügel, W.-A.; Pepin, N.; Yao, T. Review of climate and cryospheric change in the Tibetan Plateau. *Environ. Res. Lett.* **2010**, *5*, 015101. [[CrossRef](#)]
- Li, F.; Ye, Y.P.; Song, B.W.; Wang, R.S.; Tao, Y. Assessing the changes in land use and ecosystem services in Changzhou municipality, Peoples’ Republic of China, 1991–2006. *Ecol. Indic.* **2014**, *42*, 95–103. [[CrossRef](#)]
- Wang, F.; Wang, X.; Zhao, Y.; Yang, Z. Temporal variations of NDVI and correlations between NDVI and hydro-climatological variables at Lake Baiyangdian, China. *Int. J. Biometeorol.* **2014**, *58*, 1531–1543. [[CrossRef](#)] [[PubMed](#)]
- Bohnet, I.C.; Pert, P.L. Patterns, drivers and impacts of urban growth—A study from Cairns, Queensland, Australia from 1952 to 2031. *Landsc. Urban Plann.* **2010**, *97*, 239–248. [[CrossRef](#)]
- Alberti, M. The effects of urban patterns on ecosystem function. *Int. Reg. Sci. Rev.* **2005**, *28*, 168–192. [[CrossRef](#)]
- Yuan, J.; Chen, J.; Sciusco, P.; Kolluru, V.; Saraf, S.; John, R.; Ochirbat, B. Land Use Hotspots of the Two Largest Landlocked Countries: Kazakhstan and Mongolia. *Remote Sens.* **2022**, *14*, 1805. [[CrossRef](#)]
- Diogo, V.; Koomen, E.; Kuhlman, T. An economic theory-based explanatory model of agricultural land-use patterns: The Netherlands as a case study. *Agric. Syst.* **2015**, *139*, 1–16. [[CrossRef](#)]
- Chen, K.; Long, H.; Liao, L.; Tu, S.; Li, T. Land use transitions and urban-rural integrated development: Theoretical framework and China’s evidence. *Land Use Policy* **2020**, *92*, 104465. [[CrossRef](#)]
- Venkatesh, K.; Ramesh, H.; Das, P. Modelling stream flow and soil erosion response considering varied land practices in a cascading river basin. *J. Environ. Manag.* **2020**, *264*, 110448. [[CrossRef](#)]
- Wagle, N.; Acharya, T.D.; Kolluru, V.; Huang, H.; Lee, D.H. Multi-Temporal Land Cover Change Mapping Using Google Earth Engine and Ensemble Learning Methods. *Appl. Sci.* **2020**, *10*, 8083. [[CrossRef](#)]
- Feng, L.; Lei, G.; Nie, Y. Exploring the eco-efficiency of cultivated land utilization and its influencing factors in black soil region of Northeast China under the goal of reducing non-point pollution and net carbon emission. *Environ. Earth Sci.* **2023**, *82*, 94. [[CrossRef](#)]
- Costanza, R.; d’Arge, R.; deGroot, R.; Farber, S.; Grasso, M.; Hannon, B.; Limburg, K.; Naeem, S.; O’Neill, R.V.; Paruelo, J.; et al. The value of the world’s ecosystem services and natural capital. *Nature* **1997**, *387*, 253–260. [[CrossRef](#)]
- Wang, R.S.; Li, F.; Hu, D.; Li, B.L. Understanding eco-complexity: Social-Economic-Natural Complex Ecosystem approach. *Ecol. Complex.* **2011**, *8*, 15–29. [[CrossRef](#)]

27. Xu, X.Z.; Xu, Y.; Chen, S.C.; Xu, S.G.; Zhang, H.W. Soil loss and conservation in the black soil region of Northeast China: A retrospective study. *Environ. Sci. Policy* **2010**, *13*, 793–800. (In Chinese) [[CrossRef](#)]
28. Li, X.; Li, Y.; Wang, B.; Sun, Y.; Cui, G.; Liang, Z. Analysis of spatial-temporal variation of the saline-sodic soil in the west of Jilin Province from 1989 to 2019 and influencing factors. *CATENA* **2022**, *217*, 106492. [[CrossRef](#)]
29. Chang, L.; Zhao, Z.; Jiang, L.; Li, Y. Quantifying the Ecosystem Services of Soda Saline-Alkali Grasslands in Western Jilin Province, NE China. *Int. J. Environ. Res. Public Health* **2022**, *19*, 4760. [[CrossRef](#)]
30. Wang, M.; Liu, J.; Wang, J.; Zhao, G. Ecological footprint and major driving forces in West Jilin Province, Northeast China. *Chin. Geogr. Sci.* **2010**, *20*, 434–441. [[CrossRef](#)]
31. Wang, X.; Li, Y.; Chu, B.; Liu, S.; Yang, D.; Luan, J. Spatiotemporal Dynamics and Driving Forces of Ecosystem Changes: A Case Study of the National Barrier Zone, China. *Sustainability* **2020**, *12*, 6680. [[CrossRef](#)]
32. Liu, J.Y.; Kuang, W.H.; Zhang, Z.X.; Xu, X.L.; Qin, Y.W.; Ning, J.; Zhou, W.C.; Zhang, S.W.; Li, R.D.; Yan, C.Z.; et al. Spatiotemporal characteristics, patterns, and causes of land-use changes in China since the late 1980s. *J. Geog. Sci.* **2014**, *24*, 195–210. [[CrossRef](#)]
33. Xu, X.; Liu, J.; Zhang, S.; Li, R.; Yan, C.; Wu, S. *China's Multi-Period Land Use Land Cover Remote Sensing Monitoring Data Set (CNLUCC)*; Resource and Environment Data Cloud Platform: Beijing, China, 2018. [[CrossRef](#)]
34. Guo, L.Y.; Wang, D.L.; Qiu, J.J.; Wang, L.G.; Liu, Y. Spatio-temporal patterns of land use change along the Bohai Rim in China during 1985–2005. *J. Geog. Sci.* **2009**, *19*, 568–576. [[CrossRef](#)]
35. Liu, J.; Zhang, Z.; Xu, X.; Kuang, W.; Zhou, W.; Zhang, S.; Li, R.; Yan, C.; Yu, D.; Wu, S.; et al. Spatial patterns and driving forces of land use change in China during the early 21st century. *J. Geog. Sci.* **2010**, *20*, 483–494. [[CrossRef](#)]
36. Ning, J.; Liu, J.Y.; Kuang, W.H.; Xu, X.L.; Zhang, S.W.; Yan, C.Z.; Li, R.D.; Wu, S.X.; Hu, Y.F.; Du, G.M.; et al. Spatiotemporal patterns and characteristics of land-use change in China during 2010–2015. *J. Geog. Sci.* **2018**, *28*, 547–562. [[CrossRef](#)]
37. Fick, S.E.; Hijmans, R.J. WorldClim 2: New 1-km spatial resolution climate surfaces for global land areas. *Int. J. Climatol.* **2017**, *37*, 4302–4315. [[CrossRef](#)]
38. Adler, R.F.; Sapiano, M.R.P.; Huffman, G.J.; Wang, J.-J.; Gu, G.; Bolvin, D.; Chiu, L.; Schneider, U.; Becker, A.; Nelkin, E.; et al. The Global Precipitation Climatology Project (GPCP) Monthly Analysis (New Version 2.3) and a Review of 2017 Global Precipitation. *Atmosphere* **2018**, *9*, 138. [[CrossRef](#)]
39. Sun, H.; Xu, Q.; Wang, Y.; Zhao, Z.; Zhang, X.; Liu, H.; Gao, J. Agricultural drought dynamics in China during 1982–2020: A depiction with satellite remotely sensed soil moisture. *GISci. Remote Sens.* **2023**, *60*, 2257469. [[CrossRef](#)]
40. Zomer, R.J.; Xu, J.; Trabucco, A. Version 3 of the Global Aridity Index and Potential Evapotranspiration Database. *Sci. Data* **2022**, *9*, 409. [[CrossRef](#)]
41. Long, H. Land use policy in China: Introduction. *Land Use Policy* **2014**, *40*, 1–5. [[CrossRef](#)]
42. Song, Y.; Wang, J.; Ge, Y.; Xu, C. An optimal parameters-based geographical detector model enhances geographic characteristics of explanatory variables for spatial heterogeneity analysis: Cases with different types of spatial data. *GISci. Remote Sens.* **2020**, *57*, 593–610. [[CrossRef](#)]
43. Guan, D.; Gao, W.; Watari, K.; Fukahori, H. Land use change of Kitakyushu based on landscape ecology and Markov model. *J. Geog. Sci.* **2008**, *18*, 455–468. [[CrossRef](#)]
44. Wang, J.F.; Li, X.H.; Christakos, G.; Liao, Y.L.; Zhang, T.; Gu, X.; Zheng, X.Y. Geographical Detectors–Based Health Risk Assessment and its Application in the Neural Tube Defects Study of the Heshun Region, China. *Int. J. Geog. Inf. Sci.* **2010**, *24*, 107–127. [[CrossRef](#)]
45. Chen, W.; Li, J.; Zeng, J.; Ran, D.; Yang, B. Spatial heterogeneity and formation mechanism of eco-environmental effect of land use change in China. *Geogr. Res.* **2019**, *38*, 10878. [[CrossRef](#)]
46. Wang, J.; Xu, C. Geodetector: Principle and prospective. *Acta Geogr. Sin.* **2017**, *72*, 116–134. (In Chinese) [[CrossRef](#)]
47. Zhai, J.; Wang, L.; Liu, Y.; Wang, C.; Mao, X. Assessing the effects of China's Three-North Shelter Forest Program over 40 years. *Sci. Total Environ.* **2023**, *857*, 159354. [[CrossRef](#)]
48. Liu, J.; Zang, C.; Tian, S.; Liu, J.; Yang, H.; Jia, S.; You, L.; Liu, B.; Zhang, M. Water conservancy projects in China: Achievements, challenges and way forward. *Glob. Environ. Chang.* **2013**, *23*, 633–643. [[CrossRef](#)]
49. Ma, S.; Qiao, Y.-P.; Jiang, J.; Wang, L.-J.; Zhang, J.-C. Incorporating the implementation intensity of returning farmland to lakes into policymaking and ecosystem management: A case study of the Jianghuai Ecological Economic Zone, China. *J. Clean. Prod.* **2021**, *306*, 127284. [[CrossRef](#)]
50. Yuan, C.; Shang, M.; Han, Z.; Wang, J. Research on the impact of the national ecological demonstration zone on green total factor productivity: Evidence from China. *J. Environ. Manag.* **2024**, *356*, 120421. [[CrossRef](#)]
51. Yang, H. China's Natural Forest Protection Program: Progress and impacts. *For. Chron.* **2017**, *93*, 113–117. [[CrossRef](#)]
52. Liu, Z.; Lan, J. The Sloping Land Conversion Program in China: Effect on the Livelihood Diversification of Rural Households. *World Dev.* **2015**, *70*, 147–161. [[CrossRef](#)]
53. Li, W.; Wang, W.; Chen, J.; Zhang, Z. Assessing effects of the Returning Farmland to Forest Program on vegetation cover changes at multiple spatial scales: The case of northwest Yunnan, China. *J. Environ. Manag.* **2022**, *304*, 114303. [[CrossRef](#)]
54. Jiang, M.K.; Wang, Z.; Qin, W.H.; He, Z.H. Effectiveness of national priority wildlife protection in nature reserves. *J. Ecol. Rural Environ.* **2006**, *22*, 35–38+VI. [[CrossRef](#)]
55. Wang, X.; Bennett, J. Policy analysis of the Conversion of Cropland to Forest and Grassland Program in China. *Environ. Econ. Policy Stud.* **2008**, *9*, 119–143. [[CrossRef](#)]

56. Wang, Z.; Wu, J.; Madden, M.; Mao, D. China's Wetlands: Conservation Plans and Policy Impacts. *Ambio* **2012**, *41*, 782–786. [[CrossRef](#)]
57. Liu, D.; Song, C.; Fang, C.; Xin, Z.; Xi, J.; Lu, Y. A recommended nitrogen application strategy for high crop yield and low environmental pollution at a basin scale. *Sci. Total Environ.* **2021**, *792*, 148464. [[CrossRef](#)]
58. You, Y.; Zhou, N.; Wang, Y. Comparative study of desertification control policies and regulations in representative countries of the Belt and Road Initiative. *Glob. Ecol. Conserv.* **2021**, *27*, e01577. [[CrossRef](#)]
59. Fan, J.; Li, P. The scientific foundation of Major Function Oriented Zoning in China. *J. Geog. Sci.* **2009**, *19*, 515–531. [[CrossRef](#)]
60. Xie, X.; Li, X.; Fan, H.; He, W. Spatial analysis of production-living-ecological functions and zoning method under symbiosis theory of Henan, China. *Environ. Sci. Pollut. Res.* **2021**, *28*, 69093–69110. [[CrossRef](#)]
61. Qi, Q. Application of a groundwater modelling system in groundwater environmental impact assessment of river and lake connection in western Jilin region. *Appl. Ecol. Environ. Res.* **2019**, *17*, 5059–5066. [[CrossRef](#)]
62. Lu, N.; Tian, H.; Fu, B.; Yu, H.; Piao, S.; Chen, S.; Li, Y.; Li, X.; Wang, M.; Li, Z.; et al. Biophysical and economic constraints on China's natural climate solutions. *Nat. Clim. Chang.* **2022**, *12*, 847–853. [[CrossRef](#)]
63. Lv, T.; Zeng, C.; Lin, C.; Liu, W.; Cheng, Y.; Li, Y. Towards an integrated approach for land spatial ecological restoration zoning based on ecosystem health assessment. *Ecol. Indic.* **2023**, *147*, 110016. [[CrossRef](#)]
64. Niu, X.; Liao, F.; Liu, Z.; Wu, G. Spatial–Temporal Characteristics and Driving Mechanisms of Land–Use Transition from the Perspective of Urban–Rural Transformation Development: A Case Study of the Yangtze River Delta. *Land* **2022**, *11*, 631. [[CrossRef](#)]
65. Venkatesh, K.; John, R.; Chen, J.; Jarchow, M.; Amirkhiz, R.G.; Giannico, V.; Saraf, S.; Jain, K.; Kussainova, M.; Yuan, J. Untangling the impacts of socioeconomic and climatic changes on vegetation greenness and productivity in Kazakhstan. *Environ. Res. Lett.* **2022**, *17*, 095007. [[CrossRef](#)]
66. Uisso, A.M.; Tanrıvermiş, H. Driving factors and assessment of changes in the use of arable land in Tanzania. *Land Use Policy* **2021**, *104*, 105359. [[CrossRef](#)]
67. Kovács, D.D.; Amin, E.; Berger, K.; Reyes-Muñoz, P.; Verrelst, J. Untangling the Causal Links between Satellite Vegetation Products and Environmental Drivers on a Global Scale by the Granger Causality Method. *Remote Sens.* **2023**, *15*, 4956. [[CrossRef](#)]
68. Overmars, K.P.; de Koning, G.H.J.; Veldkamp, A. Spatial autocorrelation in multi-scale land use models. *Ecol. Model.* **2003**, *164*, 257–270. [[CrossRef](#)]
69. Tong, X.; Feng, Y. A review of assessment methods for cellular automata models of land-use change and urban growth. *Int. J. Geog. Inf. Sci.* **2020**, *34*, 866–898. [[CrossRef](#)]
70. Mitsuda, Y.; Ito, S. A review of spatial-explicit factors determining spatial distribution of land use/land-use change. *Landsc. Ecol. Eng.* **2011**, *7*, 117–125. [[CrossRef](#)]
71. Chakir, R.; Le Gallo, J. Predicting land use allocation in France: A spatial panel data analysis. *Ecol. Econ.* **2013**, *92*, 114–125. [[CrossRef](#)]

Disclaimer/Publisher's Note: The statements, opinions and data contained in all publications are solely those of the individual author(s) and contributor(s) and not of MDPI and/or the editor(s). MDPI and/or the editor(s) disclaim responsibility for any injury to people or property resulting from any ideas, methods, instructions or products referred to in the content.